







# pH regulates hematopoietic stem cell potential via polyamines

Sachin Kumar<sup>1,2,\*</sup> , Jeffrey D Vassallo<sup>1</sup> , Kalpana J Nattamai<sup>1</sup>, Aishlin Hassan<sup>1</sup> , Rebekah Karns<sup>3</sup>, Angelika Vollmer<sup>4</sup>, Karin Soller<sup>4</sup>, Vadim Sakk<sup>4</sup>, Mehmet Sacma<sup>4</sup> , Travis Nemkov<sup>5</sup>, Angelo D'Alessandro<sup>5</sup>  & Hartmut Geiger<sup>4,6,\*\*</sup> 

## Abstract

Upon *ex vivo* culture, hematopoietic stem cells (HSCs) quickly lose potential and differentiate into progenitors. The identification of culture conditions that maintain the potential of HSCs *ex vivo* is therefore of high clinical interest. Here, we demonstrate that the potential of murine and human HSCs is maintained when cultivated for 2 days *ex vivo* at a pH of 6.9, in contrast to cultivation at the commonly used pH of 7.4. When cultivated at a pH of 6.9, HSCs remain smaller, less metabolically active, less proliferative and show enhanced reconstitution ability upon transplantation compared to HSC cultivated at pH 7.4. HSCs kept at pH 6.9 show an attenuated polyamine pathway. Pharmacological inhibition of the polyamine pathway in HSCs cultivated at pH 7.4 with DFMO mimics phenotypes and potential of HSCs cultivated at pH 6.9. *Ex vivo* exposure to a pH of 6.9 is therefore a positive regulator of HSC function by reducing polyamines. These findings might improve HSC short-term cultivation protocols for transplantation and gene therapy interventions.

**Keywords** DFMO; *ex vivo*; HSCs; pH; polyamine

**Subject Categories** Haematology; Metabolism; Stem Cells & Regenerative Medicine

**DOI** 10.15252/embr.202255373 | Received 9 May 2022 | Revised 21 February 2023 | Accepted 3 March 2023 | Published online 21 March 2023

**EMBO Reports (2023) 24: e55373**

## Introduction

Blood cells are sustained by hematopoietic stem cells (HSCs) in a process termed hematopoiesis (Seita & Weissman, 2010; Mendelson & Frenette, 2014). Genetic manipulation of HSCs *ex vivo*, usually coupled to a subsequent transplantation, has demonstrated

a therapeutic benefit in the treatment of monogenetic diseases like bone marrow failures or to generate the next generation of CAR-T cells (Zhen *et al*, 2021). Understanding the mechanisms that regulate the function of HSCs *ex vivo* is therefore of high therapeutic value, as a limitation of a broader therapeutic use of HSCs remains the difficulty to maintain their potential *ex vivo* (Kumar & Geiger, 2017). Current clinical protocols for *ex vivo* culture of HSCs usually lead to a loss of stemness and increase in differentiation potential. There is therefore a therapeutic need for novel approaches to at least maintain HSC function upon *ex vivo* culture.

Interestingly, changes in pH can affect the relative output of erythroid, granulocyte, and megakaryocytic cells upon differentiation of CD34<sup>+</sup> human hematopoietic progenitor cells *ex vivo* (McAdams *et al*, 1997, 1998; Hevehan *et al*, 2000; Yang *et al*, 2002). Within the bone marrow (BM) niche, a mild extracellular acidosis can be accompanied by changes in pH due to the accumulation of lactic acid following anaerobic metabolism of HSCs (Simsek *et al*, 2010; Norddahl *et al*, 2011; Wang *et al*, 2014), neutrophils (Khatib-Massalha *et al*, 2020), or in leukemic conditions (Padda *et al*, 2021). pH might therefore be a physiological modifier of HSC differentiation, and likely thus also for HSC potential. While the effect of pH on HSC function has not been investigated so far, very recent publications imply a role for changes intracellular pH for epithelial cell plasticity and embryonic stem cell differentiation (Ulmschneider *et al*, 2016; Liu *et al*, 2020). Here we demonstrate that an extracellular pH of 6.9 in *ex vivo* culture, which is distinct from the commonly used pH of 7.4, results in maintenance of HSCs *ex vivo* and affects HSC size and stress. Metabolite analyses identified the polyamine pathway as a target in pH 6.9 HSCs. Pharmacological inhibition of polyamine synthesis maintained HSC potential *ex vivo* even at a pH of 7.4. Collectively, these results establish extracellular pH and the polyamine pathway as a regulator of the function of HSCs *ex vivo*, which may be further leveraged to improve *ex vivo* cultivation protocols for clinical applications.

1 Division of Experimental Hematology and Cancer Biology, Cincinnati Children's Research Foundation, Cincinnati, OH, USA

2 Pharmacology Division, CSIR-Central Drug Research Institute, Lucknow, India

3 Division of Gastroenterology, Hepatology and Nutrition, Cincinnati Children's Hospital Medical Center and University of Cincinnati, Cincinnati, OH, USA

4 Institute of Molecular Medicine, Ulm University, Ulm, Germany

5 University of Colorado Denver - Anschutz Medical Campus, Aurora, CO, USA

6 Aging Research Center, Ulm University, Ulm, Germany

\*Corresponding author. Tel: +91 522 2772550 ext 4873; E-mail: sachin.ku@cdri.res.in

\*\*Corresponding author. Tel: +49 731 50 26700; Fax: +49 731 50 26710; E-mail: hartmut.geiger@uni-ulm.de

## Results and Discussion

### Bone marrow pH is lower than in blood

HSCs reside within BM in specialized regions termed niches. Previous reports suggest there are, upon disease, tissue-specific levels of pH which are distinct from blood (Reshetnyak *et al.*, 2020). The pH range HSCs are exposed to *in vivo* is not known. Therefore, initial experiments were conducted to determine the pH within murine BM. Bone cavity showed a pH of 7.2, which is lower compared to the pH in blood (pH 7.4; Figs 1A, and EV1A and B). Additional studies using multiphoton live microscopy and a fluorescent pH-sensitive ratiometric probe, 8-hydroxypyrene-1,3,6-trisulfonic acid (HPTS, Fig EV1C and D; Ray *et al.*, 2012) demonstrated that the distribution of pH within BM is not uniform and heterogeneous (Fig EV1E and F). The analysis of selective landmarks as regions of interest (ROI) at either the bone surface or within BM including cells with likely osteoblastic and osteoclastic nature or known blood vessels (Fig EV1E and G) revealed that pH values within the BM of young mice might range from pH 6.4 to a pH of 7.8. HSC might thus, in their natural environment, be continuously exposed to a level of pH that is lower than pH 7.4, which is usually used in *ex vivo* culture medium. There is even the possibility that HSCs might reside in distinct pH niches in bone marrow. To the best of our knowledge, though it is currently not feasible to determine the position of HSCs together with the level of pH at that position in BM.

### An *ex vivo* pH of 6.9 maintains HSC function

To determine the effect of distinct levels of pH on the function of HSCs, 100 sorted LT-HSCs (Lin<sup>-</sup>Sca-1<sup>+</sup>c-Kit<sup>+</sup>CD34<sup>-</sup>Flt3<sup>-</sup> cells) from BM were exposed to a range of pH levels (6.4–7.8, Fig EV1H and I) at 3% oxygen for 2 days (40 h) and subsequently transplanted, alongside competitor cells, into primary recipient animals (Figs EV2A and 1B), and donor chimerism determined by flow cytometry (Figs 1B and EV2B). The level of chimerism in PB and BM to which donor HSCs contribute to in recipient animals in comparison to the competitor cells is an established measurement of HSC function. To determine the long-term engraftment and reconstitution potential following LT-HSC exposure *ex vivo* to pHs ranging from 6.9 to 7.8, BM cells from such primary mice were transplanted into secondary recipients (Fig EV2A), while animals receiving pH 7.4

HSC or pH 6.9 HSCs were subsequently followed in more detail, as exposure to pH 6.9 showed the highest levels of reconstitution of the pH 6.4–7.8 range tested in these experiments (Fig 1B). Noncultivated but also competitively transplanted LT-HSCs served as a reference in these experiments. LT-HSCs exposed to pH 6.9, in contrast to pH 7.4, conferred a higher level of chimerism in PB (significant) and BM (trend) in primary recipients (Fig 1C and D). The level of reconstitution driven by pH 6.9 HSCs in secondary recipients remained increased in PB as well as in BM (Fig 1F and H), now to a level that recipients from LT-HSCs cultured at pH 6.9 showed similar contribution compared to uncultured fresh LT-HSCs and significantly better than the contribution of pH 7.4 HSCs (Fig 1C, E, F and H). Animals reconstituted with HSCs exposed to a pH 6.9 showed no lineage bias and exhibited similar frequencies of T cells, B-cells, and myeloid cells in PB (Fig 1D and G) to that found in animals reconstituted by fresh, noncultured HSCs or HSCs exposed to a standard pH of 7.4. Distinct levels of pH, therefore, did not result in a different lineage differentiation potential of HSCs. Furthermore, percentages of HSC and progenitor cells (LT-HSCs, ST-HSCs, lymphoid-primed multipotential progenitor cells; LMPPs) within the primitive hematopoietic cell compartment were similar in primary recipient animals receiving pH 6.9, pH 7.4 or control HSCs (Fig 1I). There were only minor, but significant changes in secondary recipients, with the most prominent change being a reduced frequency of ST-HSCs in *ex vivo* cultivated HSCs, irrespective of whether exposed to pH 6.9 or 7.4 (Fig 1J). Exposure of HSCs to pH 6.9 did not differentially affect stem cell homing in a competitive stem cell homing assay (Fig EV2D), which excludes that the elevated level of chimerism in animals transplanted with pH 6.9 HSCs is linked to changes in homing of HSCs. Together, these results demonstrate that HSCs exposed to a pH of 6.9 for 2 days maintain their stem cell function in comparison to HSCs exposed to a pH of 7.4.

We also tested the outcome of a longer term exposure (6 days) of HSCs to distinct levels of pH. HSCs kept for 6 days *ex vivo* at either pH 6.9 or pH 7.4 presented with a significant relative reduction in their ability to contribute to chimerism in primary and secondary recipients when compared to untreated (non-cultivated) HSCs, with HSCs exposed to a pH of 6.9 with an even lower level of chimerism than HSCs cultivated at pH 7.4 (Fig EV2E–G). The influence of changes in pH on HSC function upon longer term *ex vivo* culture is thus distinct from the maintenance effect of pH 6.9 with a short-term (40 h) exposure.

#### Figure 1. A pH of 6.9 in the medium maintains HSC function.

- A pH within bone marrow in mice measured by using a 0.6 mm combination pH probe that was well calibrated with 4.00, 7.00, and 10.00 standards with  $> 0.98 R^2$  reading.  $n = 5$  or more animals from two independent experiments. Data were analyzed using two-tailed Student's *t*-test, and exact *P* values are mentioned between groups.
- B HSC (100 cells) from C57BL/6 mice (Ly5.2) were cultured under distinct pH (6.9–7.8) settings for 40 h and transplanted alongside  $2 \times 10^5$  competitor cells from Boyl mice (Ly5.1). Summary of initial screening of diverse pH effects on contribution of total donor-derived Ly5.2<sup>+</sup> cells in PB and BM in competitive primary and secondary transplants. Data are means of  $n =$  at least 14 mice per group and five experiments.
- C–J HSC (100 cells) were untreated or cultured under pH 7.4 and pH 6.9 for 40 h and transplanted with competitor cells.  $n =$  at least 18 mice per group out of at least seven experiments (biological repeats) (C, F) Contribution of donor-derived Ly5.2<sup>+</sup> cells to PB cells in primary (C) and secondary (F) recipients between 4 and 20 weeks post transplant.  $^{**}P < 0.01$ ,  $^{***}P < 0.001$  with respect to pH 7.4 treatment or between marked groups using two-tailed Student's *t*-test. (D, G) Relative contribution of T cells, B cells, and myeloid cells among PB donor-derived Ly5.2<sup>+</sup> cells in primary (D) and secondary (G) recipients at 16–20 weeks post transplant. (E, H) Contribution of donor-derived Ly5.2<sup>+</sup> cells to BM cells in primary (E) and secondary (H) recipients at 16–20 weeks post transplant.  $^{**}P < 0.01$  using two-tailed Student's *t*-test. (I, J) Representative FACS dot plots and quantitative and statistical analysis of LT-HSC, ST-HSC, and LMPP distribution among donor-derived LSKs in primary (I) and secondary (J) recipients.  $^{*}P < 0.05$  using two-tailed unpaired Student's *t*-test.

Data information: All data are means  $\pm$  SE.

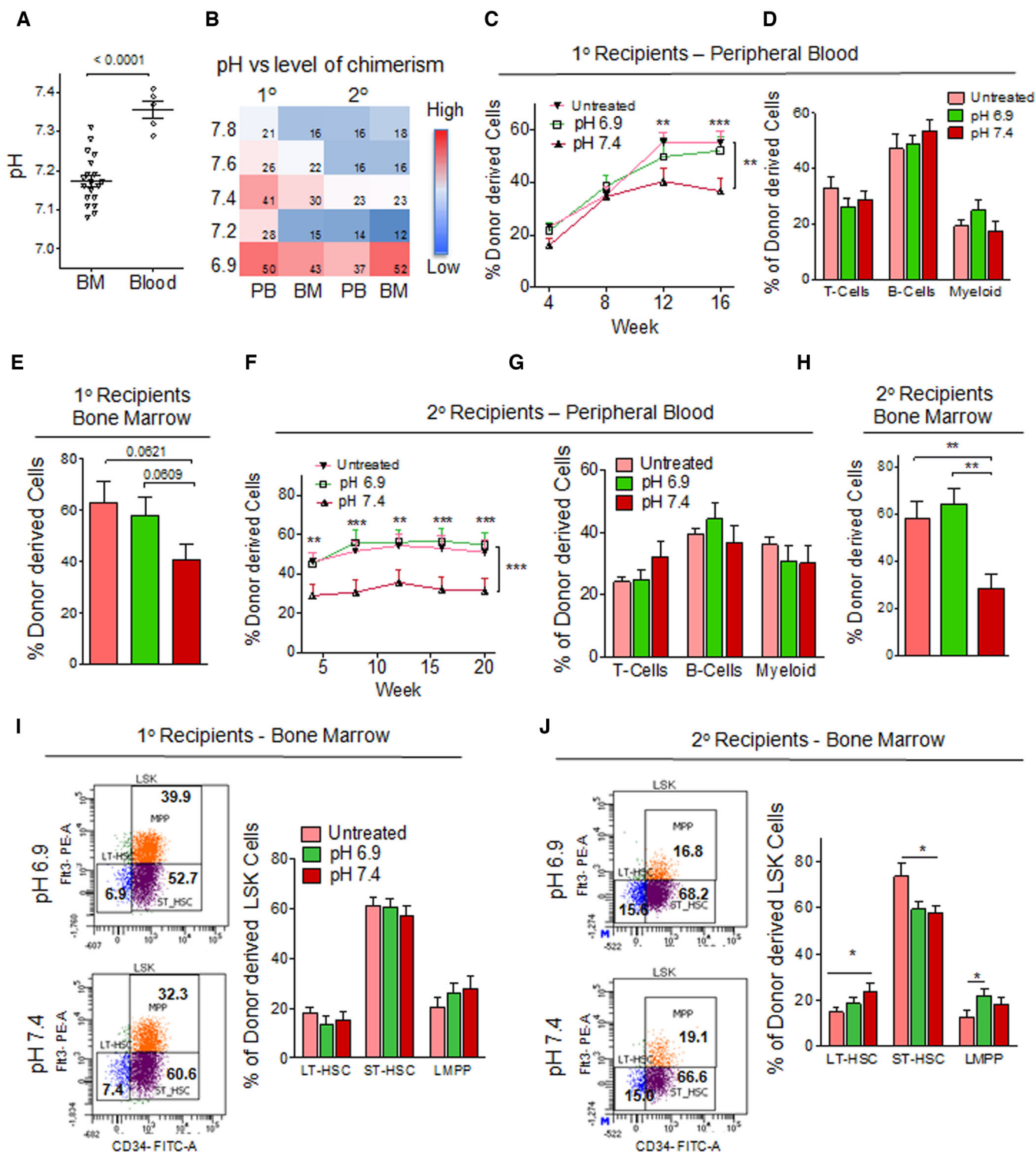


Figure 1.

To determine whether changes in pH also affect the function of hematopoietic progenitor cells (HPCs), cells from BM depleted for differentiated cells (LIN-cells) and thus enriched for progenitor cells were incubated in medium with a pH ranging from 6.9 to 8.0 for 2 days. Following incubation, the overall cell number and the HPC

activity with a colony-forming cell assay were determined. While overall numbers were highest in cells exposed to a pH of 6.9 to 7.4, their numbers dropped dramatically at higher pH (7.6–8.0) levels (Fig EV3A). Furthermore, colony-forming unit cells, using a CFU-Cs assay, were decreased at a pH of 6.9, when compared to cells

cultivated at pH 7.4 or higher (7.6–8.0; Fig EV3B). The data support that changes in extracellular pH also affect the function of HPCs. The full extent to which changes in pH will affect HPCs function will need to be further investigated.

### Extracellular pH 6.9 reduces growth, size, and metabolic stress of HSCs

Changes in the extracellular pH (pHe) have been shown to modulate the intracellular pH (pHi; Casey *et al*, 2010; Damaghi *et al*, 2013). Intracellular pH was determined using carboxy SNARF-1 as a cell-permeable fluorescent pH probe, and pH values of HSCs were calculated based on a pH-SNARF-1 standard curve (Fig EV3C–E). These data demonstrated that a pHe of 6.9 led to a decrease in pHi of HSCs (Fig EV3F) and suggest that reduced pHi levels in HSCs may contribute to the functional changes in HSCs when exposed to a pHe of 6.9. Interestingly, a pHe of 6.9 also decreased the pHi in more differentiated progenitor cells (Lin negative cells) compared to the pHi following exposure to a pHe of 7.4 (Fig EV3F).

To investigate likely mechanisms underlying the enhanced reconstitution potential of pH 6.9 HSCs, we determined the effect of pH 6.9 or 7.4 on HSC growth and proliferation. Culture of HSCs at pH 7.4 led to approximately 5-fold expansion of the cell number from HSCs, while a reduced but consistent 2-fold expansion at pH 6.9 was observed (Fig 2A). Changes in pHe have also been reported to alter cell size via altering the cytoskeleton (Busch *et al*, 1994; Kohler *et al*, 2012). While HSCs increased their size upon cultivation (Fig EV3G and H), HSC remained smaller when cultivated at pH 6.9 compared to 7.4, measured by regular microscopy, flow cytometry, and confocal imaging (Figs 2B, and EV3G and H), with a smaller nuclear volume (Figs EV3I and 4K). A smaller size of HSCs has been recently associated with an increase in stem cell potential (Lengefeld *et al*, 2021). Cell cycle analysis using standard DNA staining combined with EdU incorporation and flow cytometry implied a higher frequency of HSCs at G0/G1 phase and a lower number of HSCs entering S-phase at pH 6.9 in comparison to pH 7.4 (Fig 2C). A significantly increased frequency of cells positive for CD34, a marker associated with differentiation of murine HSCs, was observed at pH 7.4 compared to pH 6.9, which is consistent with enhanced maintenance of HSCs at pH 6.9 (Fig EV3J). Maintenance of HSC function at

pH 6.9 thus correlates with a small cell size and a reduced frequency of cycling cells.

It has been reported that in general HSCs show low levels of reactive oxygen species (ROS) in comparison to more differentiated hematopoietic cells and suggested that this low level might be important for proper HSC function (Ito *et al*, 2006; Jang & Sharkis, 2007). Additionally, it was hypothesized that changes in pH and ROS levels might be linked (Selivanov *et al*, 2008). Following exposure to pH 6.9 HSCs showed less intracellular ROS compared to pH 7.4 HSCs (Fig 2D), implying a connection between the level of pH and levels of ROS in HSCs. Ultimately though, only co-staining of pH and ROS in individual cells, which is currently technically not achievable, will be able to reveal the nature of this relationship.

HSCs also exhibit a unique cell metabolism profile. For example, in hypoxic conditions like the BM niche, Hypoxia-inducible factor 1- $\alpha$  (Hif1 $\alpha$ ) is stabilized and ATP generation is primarily glycolysis-driven (Takubo *et al*, 2010; Unnisa *et al*, 2012). At a pH of 6.9, the level of expression of the metabolic regulators phosphoinositide-dependent kinase-1 (Pdk-1) and vascular endothelial growth factor A (Vegfa) was increased in comparison to pH 7.4 HSCs (Fig 2E), while interestingly the level of Hif1 $\alpha$  expression and BCL2/adenovirus E1B 19 kDa protein-interacting protein 3 (Bnip3), a hypoxia regulated cell death protein, was not affected by changes in pH (Fig EV4A). As Hif1 $\alpha$  is primarily regulated posttranslationally and not by the level of transcription, further investigations are warranted to test the role of Hif1 $\alpha$  upon changes in pH.

Furthermore, mitochondrial function and removal of damaged mitochondria by autophagy or mitophagy have an essential role in HSC maintenance (Jin *et al*, 2018). Surprisingly, a low abundance of the autophagy markers microtubule-associated proteins 1A/1B light chain 3B (LC3) or lysosome-associated membrane protein 2 (LAMP2) was observed in HSCs exposed to a pH of 6.9 compared to 7.4 (Fig 2F and G, and Movies EV1 and EV2). This was further supported by ultrastructural analyses of HSCs. pH 6.9 HSCs displayed a reduced frequency of autophagy vacuoles and more intact mitochondria, whereas pH 7.4 HSCs presented higher levels of vacuolization and altered mitochondrial structures consistent with stress (Figs 2H and EV4F). Functional metabolic analyses revealed that a pH of 6.9 enhanced mitochondrial function in HSPCs (Fig EV4B–E) as indicated by an increase in maximum oxygen

**Figure 2. Extracellular pH regulates cell growth, size, and cellular and metabolic stress.**

- A Experimental setup for the cell growth, size and cell cycle analysis using EdU incorporation. Picture of 100 untreated HSCs or after culture under pH 7.4 or pH 6.9 conditions for 40 h. Bar graph represents cell numbers at 40 h post cultivation relative to the input (scale bar = 100  $\mu$ m,  $n = 4$  biological replicates)  $***P < 0.001$  using two-tailed unpaired Student's  $t$ -test.
- B Data representing 3D construction images depicting cell volume of HSCs cultured under pH 7.4 and pH 6.9 conditions, bar graph representing cell size distribution of HSC cultured under pH 7.4 and pH 6.9 conditions (scale bar = 20  $\mu$ m,  $n = 4$  biological replicates).
- C Representative flow cytometric analyses of EdU incorporation and DNA content in HSCs after culture under pH 7.4 and pH 6.9 conditions for 40 h. Percentage of cells in G1, S and G2/M phase of cell cycle under pH 7.4 or pH 6.9 conditions. ( $n = 4$  biological replicates,  $***P < 0.001$ ; using two-tailed unpaired Student's  $t$ -test)
- D Representative flow cytometric histogram overlay and quantification (bar graph) for intracellular ROS levels using DCF-DA in HSC after culture under pH 7.4 or pH 6.9 conditions ( $n = 4$  biological replicates,  $**P < 0.01$ ; using two-tailed unpaired Student's  $t$ -test).
- E Relative levels of expression of the Hif1 $\alpha$  transcriptional targets Pdk-1 and Vegfa ( $n = 4$  biological replicates,  $*P < 0.05$ ; using two-tailed unpaired Student's  $t$ -test).
- F, G (F) Representative image analyses of autophagy markers LC3 and LAMP2 with DAPI in HSCs after culture under pH 7.4 or pH 6.9 conditions (scale bar = 5  $\mu$ m) and (G) quantification of LC3 and LAMP2 levels. Data are from at least 50 cells representing three biological replicates.  $***P < 0.001$ ,  $****P < 0.0001$ ; using two-tailed unpaired Student's  $t$ -test.
- H Representative ultra-structural transmission electron microscopy images of untreated and cultured HSCs under pH 7.4 or pH 6.9 conditions. Data represent  $n = 20$  cells from two biological replicates. Arrows label mitochondria, while arrowheads label vacuolar structures (scale bar = 1  $\mu$ m).

Data information: All data are mean  $\pm$  SE.

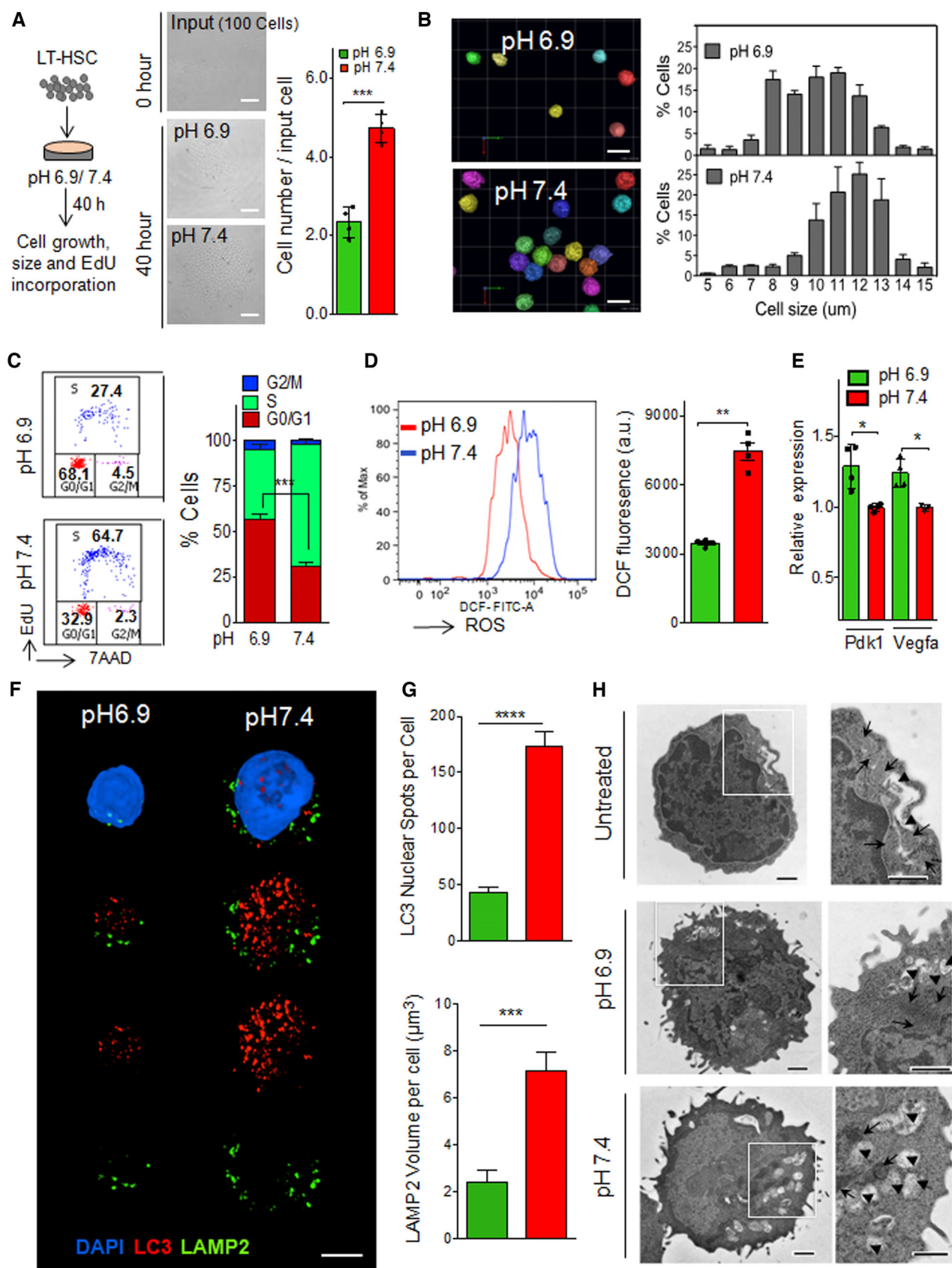


Figure 2.

consumption rate (OCR) (Fig EV4D), similar to how changes of pH affect mitochondrial function in yeast (Hughes & Gottschling, 2012).

### pH changes affect the expression of stemness genes in HSCs

RNA-seq analyses were performed on HSCs exposed to pH 6.9 and 7.4. Consistent with a difference in their function, HSCs showed a clear separation along principal components at pH 6.9 and 7.4 (Fig 3A, the PCA variability explained is 23.8% for PC1, 8.1% for PC2). We identified 838 genes differentially expressed among pH 6.9 and 7.4 HSCs (Fig 3B). Correlation with published gene-expression data sets and gene-ontology/pathway analyses on the differentially expressed gene sets revealed that the gene sets upregulated following the exposure to pH 6.9 compared to 7.4 were enriched with multiple gene signatures also upregulated in stem cells in general (referred to the adult stem cell module) and also gene sets enriched in HSCs (Fig 3C). These analyses support that exposure to a pH 6.9 affects/enhances transcriptional programs associated with stemness. The gene sets for which expression was downregulated upon pH 6.9 compared to pH 7.4 were enriched for gene signatures upregulated in progenitors but not in stem cells or untreated HSCs (Fig 3D). This implies that at pH 6.9 HSCs expression of genes associated with differentiation is suppressed. Analyses of gene ontology and biological processes of gene sets up and downregulated upon pH 6.9 compared to pH 7.4 revealed processes consistent with a low metabolic, cellular oxidation, signaling, and divisional activity (Fig 3E and F). Altogether, transcriptomic analyses revealed that changes in pH affect the expression of a large set of genes linked to maintenance of stem cell potential and a lower metabolic and oxidative state of HSCs at pH 6.9 and that multiple regulatory pathways including cell metabolism may contribute to better HSC maintenance at pH 6.9 compared to pH 7.4.

### Inhibition of the polyamine pathway at pH 7.4 mimics the effects of exposure to pH 6.9

We next determined levels of metabolites in HSCs (Reisz & D'Alessandro, 2017). A PLS-discriminant analysis (PLS-DA) for distinct metabolites identified changes in inosine and spermine as most differentially affected by pH 6.9 vs. 7.4 (Fig 4A), which was mirrored by additional changes in metabolites linked to the polyamine pathway (spermine, spermidine (SPN) and 5-methyladenosine; Fig 4B). Interestingly, uncultivated HSCs showed only very low levels of spermidine and spermine (Figs 4C and EV5B). Upon cultivation of HSCs, the levels of both spermidine and spermine increased, but to a much lower level in pH 6.9 HSC compared to pH

7.4 HSCs (Fig 4C). Literature supports a connection of pH and the polyamine pathway (Miller-Fleming *et al*, 2015; Miska *et al*, 2021). Further supporting an attenuated polyamine level in pH 6.9 HSCs, the level of expression of genes that are involved in polyamine biosynthesis (peroxisomal N(1)-acetyl-spermine/spermidine oxidase (PAOX) and spermidine synthase (SRM)) was decreased, while the level of expression of genes involved in polyamine metabolic/catabolic processes (diamine acetyltransferase 1 (SAT1) and spermine oxidase (SMOX)) was increased in pH 6.9 compared to pH 7.4 HSCs (Fig EV5A).

To further investigate the role of polyamine pathway in pH-mediated regulation of HSCs, we employed a specific and established inhibitor of ornithine decarboxylase (ODC, Fig 4D) called D, L-alpha-difluoromethylornithine (DFMO) that causes a depletion of putrescine and spermidine and which is already in clinical trials for cancer therapy (Sanderson *et al*, 2019). DFMO, at a concentration of 5 mM, resulted in a decrease in intracellular pH of HSCs cultured at pH 7.4 (Fig 4E). Further, we observed a decrease in cell number similar to the decrease in number observed for HSC at pH 6.9, when HSCs were cultivated a pH 7.4 in the presence of DFMO (Fig 4F and G). SPN, when provided at 1  $\mu$ M, reverted the growth of colonies of DFMO treated HSCs back to the level of growth observed at pH 7.4 (Fig 4G), confirming that the effect of DFMO is linked to changes in the level of SPN. DFMO decreased the cell size of pH 7.4 HSCs to a size similar to pH 6.9 HSCs, which was again reverted upon SPN supplementation (Fig 4H).

To determine the influence of the polyamine pathway on HSC function, HSCs cultivated at pH 7.4 were treated with DFMO or with DFMO and SPN together and subsequently competitively transplanted (similar to the experiments shown in Fig 1). DFMO-treated HSCs showed improved *ex vivo* maintenance, as determined by an elevated chimerism in both primary and secondary recipients in blood as well as in BM (Fig 4I and J). DFMO-treated pH 7.4 HSCs also resembled to a large extent pH 6.9 HSCs with respect to the low level of LAMP2 seen in pH 6.9 HSCs as well as in untreated HSCs (Figs 4K and 2F). The positive influence of pH 6.9 or DFMO on HSC was not restricted to fetal bovine serum (FBS) containing medium or to murine HSCs. Both murine HSCs as well as human HSPCs (CD34<sup>+</sup> cells that are directly applied in clinical transplantation protocols) cultivated in a standard serum-free medium used in clinical protocols (STEMSpan) and exposed for 2 days to pH 6.9 or 7.4 cells cultivated with DFMO also showed lower cell numbers after 2 days compared to pH 7.4 exposed cells (Fig EV5C and D), which was identical to what we observed for murine HSCs cultivated with FBS-containing medium (Figs 2A and 4G). Upon transplantation or xenotransplantation (human HSPCs), pH 6.9 murine HSCs or human HSPCs showed a level of chimerism that was significantly improved

**Figure 3. pH affects HSC gene expression profiles.**

- A PCA analysis plots of log<sub>2</sub>-normalized FPKM of six RNA-seq samples for HSCs cultured under pH 7.4 or pH 6.9 conditions (*n* = 6 biological replicates).
- B Hierarchical clustering and heatmap representing global visualization of all the DEGs in HSCs present at pH 6.9 or pH 7.4 for 40 h (*n* = 6 biological replicates). Results were visualized using Treeview.
- C Correlation of DEGs with published gene-expression data sets that were upregulated at pH 6.9 treatment (*n* = 6 biological replicates).
- D Correlation of DEGs with published gene-expression data sets that were downregulated at pH 6.9.
- E, F (E) GO biological process analyses depicting altered processes greater than 0.5-fold up at pH 6.9 and (F) the processes decreased at pH 6.9. DEGs were imported in Cytoscape and clustered using ClueGO plugin for Gene Ontology. Respective groups were collected posttreatment and subjected to RNA-seq. Log<sub>2</sub> values were used to cluster and generate Treeview. *n* = 6 biological replicates.

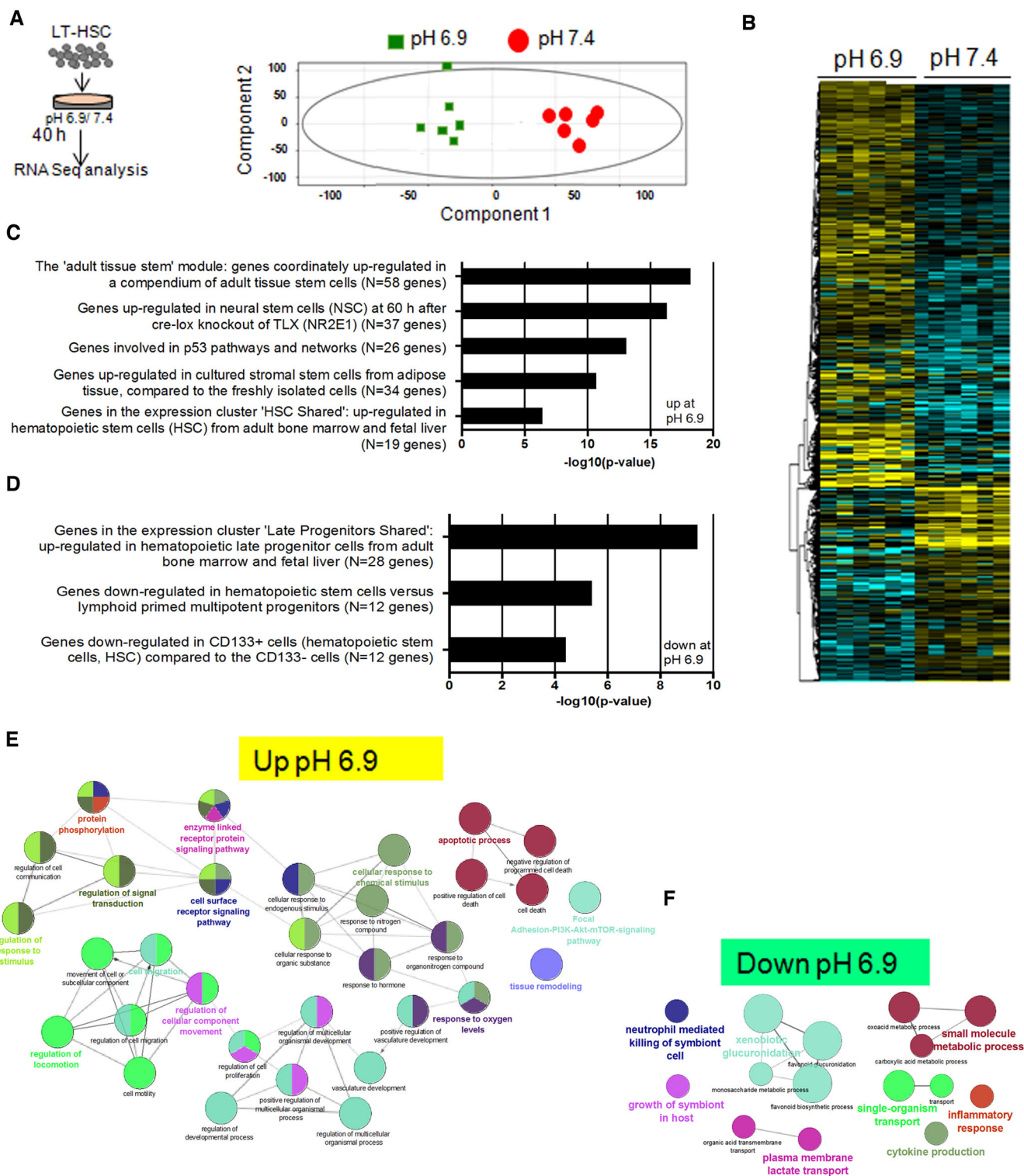


Figure 3.

compared to pH 7.4 HSCs/human HSPCs, with DMFO-treated HSCs/human HSPCs showing a trend of improved function compared to pH 7.4 exposed cells and supporting a level of chimerism very similar to untreated/uncultivated fresh cells (Fig 4L). Murine pH 6.9 and

especially 7.4+ DMSO HSCs, whether cultivated for 2 days with or without serum, showed elevated levels of apoptosis when compared to pH 7.4 HSCs, which might, besides the reduced number of cells in S-phase (Fig 2C), contribute to the lower number of cells seen

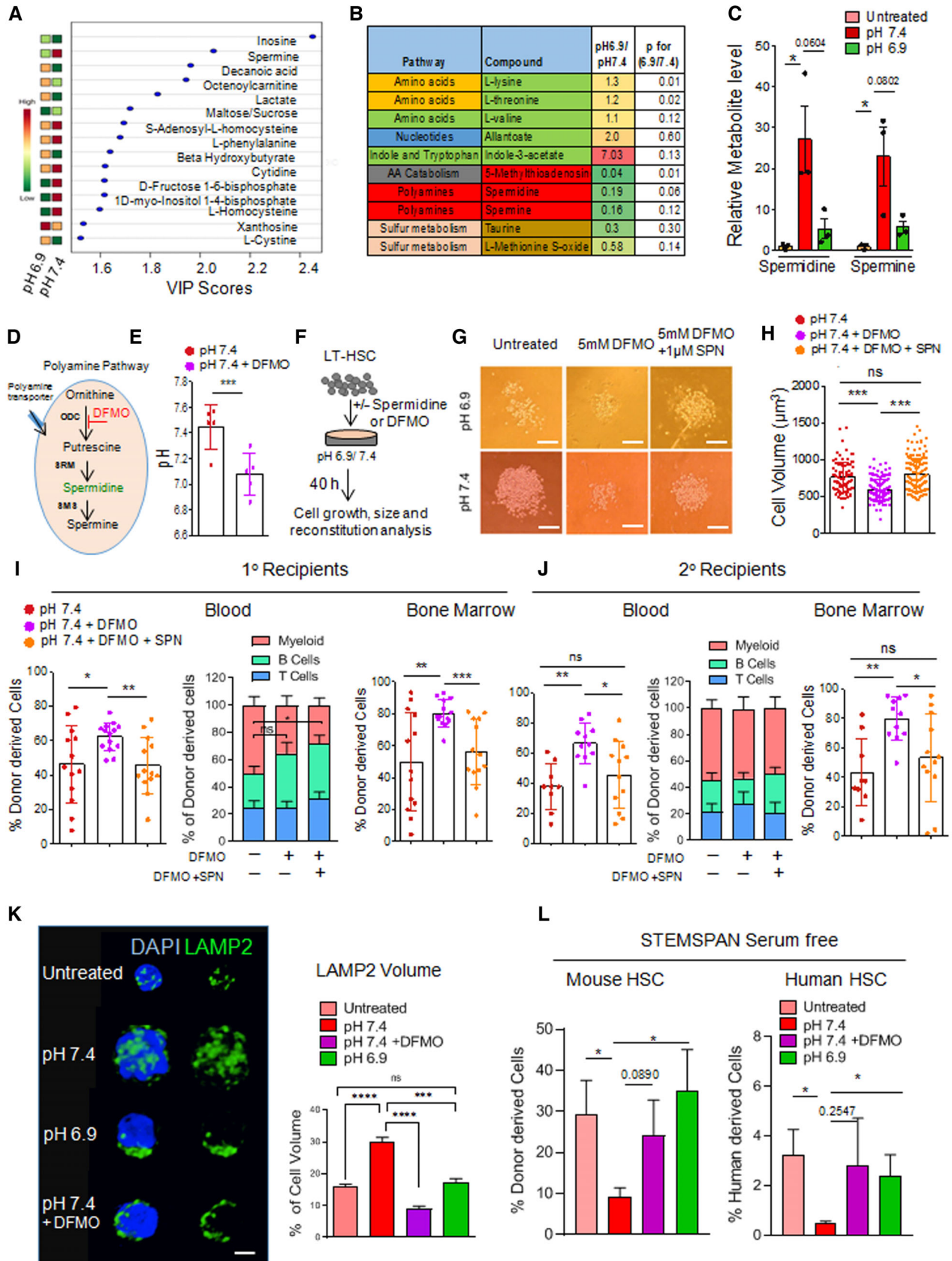


Figure 4.



**Figure 4. pH regulates HSC potential via polyamines.**

- A VIP scores of key metabolites altered in HSCs after culture under pH 7.4 or pH 6.9 conditions.  $n = 3$  biological replicates.
- B Table representing major pathways and metabolite median changes in HSCs at pH 6.9 with respect to pH 7.4 condition.  $n = 3$  biological replicates.
- C Relative levels of spermidine and spermine in pH 6.9 and pH 7.4 conditions with respect to untreated samples.  $n = 3$  biological replicates.  $*P < 0.05$  and exact  $P$  values are mentioned between groups.
- D Schema represents polyamines pathway with key intermediates, enzymes and ornithine decarboxylase (ODC) as the DFMO target.
- E Effect of DFMO treatment on pH<sub>i</sub> of HSCs.  $n = 5$  biological replicates.  $***P < 0.001$  using two-tailed unpaired Student's  $t$ -test.
- F Experimental set-up for the determination of cell growth, size, and reconstitution analysis of HSCs upon modulation of the polyamine pathway using DFMO and DFMO/spermidine (SPN) treatment.
- G Pictures of HSCs after culture at pH 7.4 or pH 6.9 and in presence or absence of DFMO and SPN for 40 h. Data are representative of six biological replicates. Scale bar = 100  $\mu$ m.
- H Cell volume of HSCs cultured at pH 7.4 in the presence of DFMO or in combination with SPN. Data are from > 80 cells per group, representative of three biological replicates.  $***P < 0.001$  using two-tailed unpaired Student's  $t$ -test.
- I, J Reconstitution level of donor-derived Ly5.2<sup>+</sup> cells,  $\gamma$ -lineage distribution in peripheral blood and BM in primary (I) and secondary (J) recipients from 100 HSCs cultured at pH 7.4 in presence of DFMO or in combination of SPN. Data in fig (I, J) are from  $n = 9$ –12 recipient mice from two independent biological transplantation experiments.  $*P < 0.05$ ,  $**P < 0.01$ ,  $***P < 0.001$  using two-tailed unpaired Student's  $t$ -test.
- K Representative images of autophagy markers LAMP2 with DAPI in untreated HSCs or after culture under pH 6.9, pH 7.4, or pH 7.4 in presence of DFMO (scale bar = 5  $\mu$ m). Bar graphs represent quantification of LAMP2 levels in cells. Data are from > 50 cell representing three biological replicates.  $***P < 0.001$ ,  $****P < 0.0001$  using two-tailed unpaired Student's  $t$ -test.
- L Reconstitution level of donor-derived Ly5.2<sup>+</sup> cells or human-derived cells in peripheral blood in primary recipients from either untreated 100 murine or human HSCs or after culture in serum-free medium STEMspan under pH 6.9, pH 7.4, or pH 7.4 in presence of DFMO.  $n = 7$ –9 mice from two biological transplantation experiments for murine HSC data. For human HSPC transplants,  $n = 6$  recipients per condition from three biological transplantation experiments.  $*P < 0.05$ , or exact  $P$  value mentioned between groups. Statistic significance was calculated using two-tailed unpaired Student's  $t$ -test.

Data information: Columns are means  $\pm$  SE.

under the pH 6.9/pH 7.4+ DFMO conditions (Fig EV5E). While there was no difference in the level of apoptosis among the different cultivation conditions for human HSPCs (Fig EV5F), they also show a clear difference in cell number upon pH 6.9 or pH 7.4+ DFMO (Fig EV5D). The role of apoptosis for the reduced expansion of HSCs or human HSPCs at pH 6.9 or pH 7.4+ DFMO might thus likely be limited. In summary, our data support that pH 6.9 maintains murine and human HSC potential upon 2 days of *ex vivo* cultivation, most likely via attenuating polyamine production and thus polyamine levels in activated/cultivated HSCs.

In this study, we demonstrate that exposure to a pH of 6.9 instead of the commonly used pH of 7.4 for 2 days *ex vivo* results in the maintenance of murine HSC and human HSPCs function similar to level of fresh, uncultured HSCs/HSPCs. A difference in pH of 0.5 units alters the concentration of protons in the medium already by 5-fold. Interestingly, the response of HSCs to a change in pH is not linear (Fig 1B). One possibility might be that distinct sets of proteins within or on HSCs that are critical for stem cell potential show distinct isoelectric points and thus distinct activities upon changes in pH. Changes in pH will then affect such proteins very distinctly and might also explain the low HSC potential upon exposure to pH 6.4–6.6. Modulation of the charge and the structure of macromolecules like proteins via protons ( $H^+$ ) might of course also contribute to the changes in HSC outcome (Casey *et al*, 2010). Further research will be required to better understand how minor changes in extracellular pH are able to affect HSC function in general and with respect to affecting the polyamine pathway in HSCs.

Our analyses also confirm a lower pH in BM compared to blood and pH is likely heterogeneously distributed which implies pH pockets in BM, as already previously suggested (Miettinen *et al*, 2012; Reshetnyak *et al*, 2020). It remains a possibility that HSCs reside in distinct “pH spots” in BM *in vivo* and in spots with a pH lower than pH 7.4 (Ray *et al*, 2012). Extracellular pH has previously been shown to regulate bone homeostasis. There is high osteoblastic activity at neutral pH that induces bone formation, while resorption

due to osteoclast activation is linked to a low pH (Arnett, 2003), so the function of putative pH spots, pockets, or zones in bone might be manifold. However, the hypothesis of regulatory pH pockets in BM that affect HSC function will need to await further confirmation, as it is to the best of our knowledge currently technically not feasible to combine HSC identification and pH measurements directly in BM *in vivo*.

A change in pH elicited changes in intracellular pH and in multiple signaling networks known to be able to regulate HSC function and cellular metabolism, which at the end resulted in an enhanced stem-cell like transcriptome of HSCs exposed to a pH of 6.9. Recent studies have revealed that a definite and dynamic metabolic programming is essential for proper stem cell function (Suda *et al*, 2011; Yu *et al*, 2013; Ito & Suda, 2014). Similarly, low cellular and mitochondrial stress are associated with better stem cell function (Ito *et al*, 2006; Jang & Sharkis, 2007) and observed in HSCs cultivated at pH 6.9. Moreover, a recent study identified that small-sized HSCs from mice or humans exhibit better stem cell potential (Lengefeld *et al*, 2021). pH 6.9 HSCs also remained smaller in size compared to pH 7.4 HSCs. Low cellular oxidation, small size, stabilized metabolism, reduced stress, and attenuated proliferation in HSCs have been individually linked to the maintenance of HSC potential (Ito *et al*, 2006; Jang & Sharkis, 2007; Rossi *et al*, 2012; Lengefeld *et al*, 2021), which are now observed in combination in pH 6.9 HSCs.

An extracellular pH of 6.9 for 2, but not 6 days, resulted in maintenance of HSC function and reconstitution ability. A 2-day *ex vivo* cultivation of HSCs is required for successful gene therapy protocols (Morgan *et al*, 2017; Ribeil *et al*, 2017), while HSCs or HSPCs already lose some of their potential within such cultivation protocols (Figs 1F and H, and 4L). The maintenance of the potential *ex vivo* might thus already be sufficient to contribute to a significantly improved outcome for such protocols. Our data indicate that a lower frequency of *ex vivo* divisions of HSCs at pH 6.9 or in the presence of DFMO might contribute to their enhanced repopulation ability. For HSC expansion in culture, HSCs need to change the

mode of divisions (asymmetric to symmetric) and show strong proliferation. As the likely mode of action of pH 6.9 though is a low frequency of HSC divisions and changes in a panel of metabolic processes in the short-term 2-day culture, the reduction in reconstitution potential upon 6 days of *ex vivo* culture might owe, in a two-edged sword fashion, to the underlying mechanism that maintains function when HSCs are cultivated for short term (2 days).

Our transcriptional and metabolite analyses identified the polyamine pathway as a mechanism of maintaining HSC potential at pH 6.9, and that level of polyamines is significantly increased in HSCs upon their activation/cultivation. Polyamines regulate, among others, translation rates and are thus essential for cell proliferation (Dever & Ivanov, 2018; Puleston *et al*, 2021). In a recent study, polyamine intermediate N1-acetylspermidine was found to regulate hair follicle stem cell fate in organoid cultures (Allmeroth *et al*, 2021). Interestingly, stem and progenitor cells can represent different polyamine levels and polyamine-mediated effects (Allmeroth *et al*, 2021). As high translation rates promote stem cell differentiation, it is surprising that elevated polyamine levels were supposedly linked to stem cell maintenance (James *et al*, 2018), which would be also in contrast to our findings. Moreover, spermidine was found to be associated with lifespan extension when supplemented in the food supply of yeast, flies, and worms in mM range (Eisenberg *et al*,

2009), though primarily via influencing the microbiome composition of the gut. In our studies, inhibition of the polyamine pathway by the drug DFMO, when provided at a pH of 7.4, mirrored to a large extent exposure of HSCs to a pH of 6.9. Recent literature supports buffering of pH by the polyamine pathway (Miller-Fleming *et al*, 2015; Miska *et al*, 2021), and indeed our finding suggests DFMO mediates a decrease in intracellular pH in HSCs. The detailed mechanisms on how a low intracellular pH and low polyamines affect HSC growth and metabolic conditions and their causal, maybe reciprocal interrelationship, need further investigations. Moreover, our data do not unequivocally claim that the effect of distinct levels of pH on reconstitution is solely stem cell intrinsic. It is formally a possibility that during the culture period stem and progenitor cells that result from stem cell expansion will also affect HSC function extrinsically.

Collectively, this work demonstrates that a simple, short-term exposure to a pH of 6.9 instead of the standard of 7.4 maintains HSC function *ex vivo*. Therefore, a pH of 6.9 in media might thus be favorable for *ex vivo* maintenance protocols. A short-term, one- to two-day *ex vivo* culture period is frequently used for viral transduction or other manipulation protocols for HSCs, both in basic science as well as in clinical settings. Our data may therefore further improve HSC cultivation protocols for HSC transplantations.

## Materials and Methods

### Reagents and Tools table

Reagent/Resource	Reference or Source	Identifier or Catalog Number
<b>Experimental models</b>		
C57BL/6] ( <i>M. musculus</i> )	Jackson Lab	B6.129P2Gpr37tm1Dgen/]
Boyl] (CD45.1) mice	Jackson Lab	B6.SJL-Ptprca Pepcb/Boyl]
NBSGW mice	Jackson Lab	NOD.Cg-KitW-41] Tyr + Prkdcscid Il2rgtm1Wjl/Thom]
<b>Antibodies</b>		
anti-CD11b	eBioscience	clone M1/70
anti-B220	eBioscience	clone RA3-6B2
anti-CD5	eBioscience	clone 53-7.3
anti-Gr-1	eBioscience	clone RB6-8C5
anti-Ter119	eBioscience	13-5921-82
anti-CD8a	eBioscience	clone 53-6.7
anti-Sca-1	eBioscience	clone D7
anti-c-Kit	eBioscience	clone 2B8
anti-CD34	eBioscience	clone RAM34
anti-Flk2	eBioscience	clone A2F10
Biotin Mouse Lineage Panel	BD Biosciences	Cat # 559971
Streptavidin-APC-Cy7	BD Biosciences	Cat # 554063
Streptavidin, AF 700	ThermoFisher	Cat # S21383
CD34-FITC, clone RAM34	eBioscience	Cat # 11-0341-82
Flt-3 PE	eBioscience	Cat # 12-1351-82
C-KIT-APC	eBioscience	Cat # 17-1171-82
Sca-1 PE-Cy7	eBioscience	Cat # 25-5981-82

Reagents and Tools table (continued)

Reagent/Resource	Reference or Source	Identifier or Catalog Number
cKit-APC-Cy7	eBioscience	Cat # A15423
CD45.2 – FITC	Biolegend	Cat # 109806
CD45.1 – PE	eBioscience	Cat # 12-0453-82
anti-CD3e- PE-Cy7	Biolegend	Cat # 100320
anti human CD45 VioBlue clone 5B1	Miltenyi	Cat #130-113-684
Mouse anti- human CD34 clone 581	BD Biosciences	Cat # 555824
FITC Rat Anti Mouse CD45 clone 30-F11	BD Biosciences	Cat # 553080
Human Hematopoietic Lineage Antibody Cocktail, FITC	eBioscience™	Cat# 22-7778-72
Anti-Human CD2 (RPA-2.10) FITC		
Anti-Human CD3 (OKT3) FITC		
Anti-Human CD14 (61D3) FITC		
Anti-Human CD16 (CB16) FITC		
Anti-Human CD19 (HIB19) FITC		
Anti-Human CD56 (TULY56) FITC		
Anti-Human CD235a (HIR2) FITC		
anti-LAMP2 antibody, GL2A7	Abcam	Cat # ab13524
Anti LC3A/B	Cell Signalling	Cat # 4108
anti-rat DyLight488-conjugated antibody	Jackson ImmunoResearch	Cat # 112-485-071
<a href="#">anti-Rabbit Alexa Fluor 555</a>	Invitrogen	Cat # A32794
PE Annexin V Apoptosis Detection Kit	BD Biosciences	Cat # 559763
<b>Chemicals, Enzymes and other reagents</b>		
Antifade Mounting Media	VECTASHIELD Laboratories	Cat # H-1000-10
8-hydroxypyrene-1,3,6-trisulphonic acid	Sigma aldrich	Cat # H1529
carboxy SNARF-1 AM	ThermoFisher	Cat # C1272
Heat-Inactivated Fetal Bovine Serum	GIBCO	Cat# 10438-026
70 kDa Rhodamine B–dextran	Life Technologies	Cat # D1841
DCF-DA	Invitrogen	Cat # D399
Click-iT Plus EdU AF488 Assay Kit	Thermo Fisher	Cat # C10420
Cell tracker green, CMFDA	Invitrogen	Cat # C2925
Cell tracker orange, CMRA	Invitrogen	Cat # C34551
XF96 plate	Agilent	Cat # 101085-004
Cell-Tak	Corning	Cat # 354240
XF Cell Mito Stress Test Kit	Agilent	Cat # 103015-100
Glycolysis Stress Test kit	Agilent	Cat # 103020-100
RNeasy Micro Kit	QIAGEN	Cat # 74004
High-Capacity cDNA RT Kit	Applied Biosystems	Cat # 4368814
SMART-Seq v4 Ultra Low Input RNA kit	Clontech	Catalog # 634892
Nextera XT DNA Library Preparation kit	Illumina	Catalog # FC-131-1096
Pyramid tip mold	Ted Pella	Cat # 10585
Cytofix Fixation Buffer	BD Biosciences	Cat # 554655
Donkey Serum	Sigma	Cat # 566460
Iscove modified Dulbecco medium (IMDM)	Cellgro	Cat#21-020-CV
MethoCult™ GF M3434	Stem Cell Technologies	Cat # 03434
Penicillin/Streptomycin	Corning	Cat# 30-002-CI
Stemspan SFEM Medium	Stemcell Technologies	Cat# 09650
Histopaque 1083	Sigma	Cat# 10831
DAPI	ThermoFisher	Cat # D1306

Reagents and Tools table (continued)

Reagent/Resource	Reference or Source	Identifier or Catalog Number
Nigericin	Sigma	Cat # N7143
NaCl	Sigma	Cat # S7653
CaCl <sub>2</sub>	Sigma	Cat # C3306
KCl	Sigma	Cat # P5405
MgCl <sub>2</sub>	Sigma	Cat # M2670
HCl	Sigma-Merck	Cat # H1758
Glucose	Sigma	Cat # G7528
NaOH		Cat # S8045
Paraformaldehyde	EMS	Cat # 15713
Glutaraldehyde	EMS	Cat # 16220
Evans blue	Sigma	Cat # E2129
Osmium tetroxide	Sigma	Cat # 75632
LX-112 resin	LADD Research	Cat # 21310
Triton X-100	Sigma	Cat # T8787
7AAD	Life Technologies	Cat # A1310
<b>Cytokines</b>		
Mouse stem cell factor	Prospec	CYT-275
Murine thrombopoietin	Prospec	CYT-346
Human recombinant G-CSF	Amgen	Neupogen 300 µg/ml
Human Recombinant TPO	Stemcell Technologies	78210
Human Recombinant IL-3	Stemcell Technologies	78040
Human Recombinant IL-6	Stemcell Technologies	78050
Human Recombinant SCF	Stemcell Technologies	78062
Human Recombinant Flt3/Fik-2 Ligand	Stemcell Technologies	78009
<b>Software</b>		
GraphPad Prism7.0	<a href="https://www.graphpad.com">https://www.graphpad.com</a>	
<b>Other</b>		
Illumina's Nextera XT DNA Library Preparation	Illumina	
96-well round bottom plates (TPP Tissue culture plates)	Midwest Scientific	TP92097
96-well flat bottom plates	suspension Sarstedt	Cat # 83.3924

## Methods and Protocols

### Experimental animals

Young female C57BL/6J (CD45.2) mice (10–12-week old) and BoyJ (CD45.1) mice (8–12-week old) and NBSGW animals were bred and housed in mouse facility at Cincinnati Children's Hospital Medical Center (CCHMC), Cincinnati, USA. The mice were housed in standard cages at 22°C under a 12–12 h light–dark cycle in a barrier facility with ad libitum access to water and food. All experimental procedures were approved by the Institutional Animal Committee at CCHMC, Cincinnati, USA. Human bone marrow mono-nucleated cells (BM MNCs) were obtained from the Translational Trials Development and Support Laboratory (TTDSL) at CCHMC.

### pH measurements inside BM

A combination glass pH probe (0.6 mm in diameter, Specialty Sensor LLC) was precalibrated using pH 4.00, 7.00, and 10.00

standards. Calibration of the electrode was done before each measurement to minimize any electrode drift (Mortensen *et al*, 1998). The precalibrated combination glass pH probe (0.6 mm in diameter, Specialty Sensor LLC) was introduced into the femoral marrow of anesthetized mice after trimming of femoral bonehead and with three axis-controlled movement setup. A box with a grounding loop was used to avoid interference. pH readings were recorded for at least 2 min, and peripheral blood pH was measured in left ventricle of heart (Mortensen *et al*, 1998).

### Calibration of pH in medium

Iscove-modified Dulbecco medium (IMDM; Cellgro), 20 ml containing 10% FBS & PS was added to 50 ml tubes, pH was set with 1 M HCl or 1 M NaOH using a pre-calibrated pH Meter (Toledo) to values based on preliminary data to get a desired pH level after over night calibration. Media was filtered with 0.22 µm and incubated overnight in at 37°C under 3% O<sub>2</sub> and 5% CO<sub>2</sub>

settings. Next day, these precalibrated media with stable and distinct pH values were used to culture. pH of Stemspan SFEM Medium (Stemcell Technologies; 09650) was calibrated similarly.

### Culture conditions

Murine HSCs or lineage negative ( $\text{Lin}^-$ ) cells were cultured under 37°C, 5%  $\text{CO}_2$ , 3%  $\text{O}_2$  conditions in IMDM containing 10% FBS & PS precalibrated for distinct pH in the presence of cytokines (SCF, TPO (Prospec CTY275, CYT-346) and G-CSF (Neupogen 300  $\mu\text{g}/\text{ml}$ , Amgen)) at 50 ng/ml concentration each. Cells were cultured at pH 6.9 or pH 7.4 +/- DFMO (Sigma) 5 mM or +/- SPN (Sigma) 1  $\mu\text{M}$  for 2 or 6 days in 96 well-round bottom plates (TPP Tissue culture plates, Midwest Scientific TP92097). In some experiments, murine HSCs were also cultured in Serum-free STEMspan SFEM medium (Stemcell Technologies; 09650) with distinct pHs or in the presence of DFMO. Human HSPCs (sorted  $\text{lin}^{\text{neg}}$   $\text{CD34}^{\text{pos}}$   $\text{SSC}^{\text{low}}$  cells from BM, anti-CD34 clone 581 (BD #555824), human hematopoietic lineage antibody cocktail, FITC, eBioscience (#22-7778-72)) were incubated in serum-free STEMspan SFEM medium (Stemcell Technologies; 09650) supplemented with cytokines (huIL3 (10 ng/ml), huIL6 (50 ng/ml), huFlt3 (20 ng/ml), huSCF and huTPO (both 100 ng/ml), all Stemcell Technologies) under hypoxic (3%  $\text{O}_2$ ) conditions in 96-well flat bottom plates (suspension Sarstedt #83.3924). Half of the cultivation media was replaced every 24 h of culture with medium of the same precalibrated pH and also containing all the cytokines and the compounds like DFMO or SPN.

### Colony-forming unit (CFU) assay

For measurement of pH effects on CFUs, MethoCult™ GF M3434 (Stem Cell Technologies) containing complete methylcellulose-based medium for colony-forming unit (CFU) assays was utilized as previously described (Ryan *et al*, 2010). Samples were plated in triplicate in six-well plates, and colonies with more than 50 cells were counted between days 7 and 10 after plating.

### Flow cytometry and cell sorting

Low-density mononuclear cells were isolated by density centrifugation (Histopaque 1083, Sigma) and stained with a cocktail of biotinylated lineage antibodies all rat anti-mouse antibodies: anti-CD11b (clone M1/70), anti-B220 (clone RA3-6B2), anti-CD5 (clone 53-7.3) anti-Gr-1 (clone RB6-8C5), anti-Ter119 and anti-CD8a (clone 53-6.7; eBioscience). After lineage depletion by magnetic separation (Dynabeads, Invitrogen), cells were stained with anti-Sca-1 (clone D7), anti-c-Kit (clone 2B8), anti-CD34 (clone RAM34), anti-Flk2 (clone A2F10), and Streptavidin antibodies (eBioscience). Stained HSCs (gated as  $\text{Lin}^- \text{Sca}^+ \text{Kit}^+ \text{CD34}^- \text{Flk2}^-$ ) were sorted in 96 well plates using a BD FACS Aria II (BD Bioscience) as previously reported (Florian *et al*, 2012). Human BM MNCs were enriched using standard Ficoll-based density centrifugation in the clinical laboratory at CCHMC. Human HSPCs ( $\text{lin}^{\text{neg}}$   $\text{CD34}^{\text{pos}}$   $\text{SSC}^{\text{low}}$  cells from BM) were FACS-sorted (BD Aria II, BD Bioscience) according to standard protocols (sorted  $\text{lin}^{\text{neg}}$   $\text{CD34}^{\text{pos}}$   $\text{SSC}^{\text{low}}$  cells from BM, anti-CD34 clone 581 (BD #555824)), human hematopoietic lineage antibody cocktail, FITC, eBioscience (#22-7778-72; Kumar *et al*, 2021).

### Competitive transplantation and reconstitution analysis

Murine HSCs (100 cells) from C57BL/6 mice ( $\text{Ly5.2}^+$ ) were cultured under diverse pH conditions or with pH 7.4 in presence of DFMO

(5 mM) or with SPN (1  $\mu\text{M}$ ) for 40 h in IMDM medium at 37°C (5%  $\text{CO}_2$ , 3%  $\text{O}_2$ ). After incubation cells were harvested and washed twice in PBS. In the untreated group, sorted HSCs were transplanted without any further incubation. HSCs were mixed with  $1.5 \times 10^5$  BM cells from young (2- to 3-month-old) BoyJ competitor mice ( $\text{Ly5.1}^+$ ) and then transplanted into lethally irradiated young BoyJ recipient mice ( $\text{Ly5.1}^+$ ). The reconstitution potential was analyzed as donor-derived chimerism in PB and BM at 4–20 weeks using immunostaining and analyzed on a CantoIII flow cytometer (BD Biosciences). Primary transplanted mice were sacrificed after 8–20 weeks and BM chimerism was determined by FACS analysis. For secondary transplants,  $3 \times 10^6$  BM cells from an individual primary recipient mouse were injected into an individual secondary, lethally irradiated recipient BoyJ mouse. All BM transplantation experiments were repeated three to six times with a cohort of four or five recipient mice per donor. For transplantation of human HSPCs, the content of a well in which 5,000 human HSPC were sorted was harvested after incubation in the distinct SFM conditions, washed twice in PBS and transplanted into busulfan conditioned NBSGW mice (10 mg/kg 48 h prior transplantation). For the untreated group in the experiments, sorted human HSPCs were directly transplanted into conditioned NBSGW recipients without any further incubation as per approved protocol IACUC2020-0075.

### Flow cytometry analysis of donor-derived chimerism

PB and BM cell immunostaining was performed according to standard procedures, and samples were analyzed on a CantoIII flow cytometer (BD Biosciences). Lineage FACS analysis data are plotted as the percentages of  $\text{B220}^+$ ,  $\text{CD3}^+$ , and myeloid ( $\text{Gr-1}^+ \text{Mac-1}^+$ ) cells among donor-derived  $\text{Ly5.2}^+$  cells, gated on viable cells based on FSC/SSC, following doublet discrimination. For early hematopoiesis analysis, Lin-cells were then stained as aforementioned and analyzed using a CantoIII flow cytometer (BD Biosciences). LT-HSCs and progenitors FACS analysis data were plotted as the percentage of LT-HSC (gated as  $\text{LSK} \text{CD34}^- / \text{lowFlk2}^-$ ), ST-HSC (gated as  $\text{LSK} \text{CD34}^+ \text{Flk2}^-$ ), and LMPP (gated as  $\text{LSK} \text{CD34}^+ \text{Flk2}^+$ ) distribution among donor-derived LSKs ( $\text{Lin}^- \text{c-Kit}^+ \text{Sca-1}^+$  cells; Florian *et al*, 2012). Primary transplanted mice were regarded engrafted when PB chimerism was greater or equal to 1.0% and contribution was detected in all lineages. Secondary transplanted mice were regarded as engrafted when PB chimerism was greater or equal to 0.5% and contribution was detected in all three cell lineages. For human HSC reconstitution analyses, 8 weeks post-transplant BM aspirates were analyzed using FACS analysis. Cells were gated on viable cells based on the FSC/SSC, and following doublet discrimination, cells negative for murine CD45 and positive for human CD45 were identified as donor-derived human cells (anti-murine CD45 clone 30-F11 BD #553080, anti-human CD45 VioBlue clone 5B1 Miltenyi #130-113-684).

### Homing assay

After pH treatment, HSCs (5,000 cells) were labeled with the cell tracker Cell tracker green, CMFDA (Invitrogen-Molecular probes) or the cell tracker orange, CMRA (Invitrogen-Molecular probes), washed, and mixed, injected into individual irradiated recipient mice. After 16 h from the HSCs injection, recipient mice were sacrificed and BM cells were analyzed by flow cytometry to quantify relative frequency of  $\text{CMFDA}^+$  and  $\text{CMRA}^+$  cells. The relative homing

to bone marrow in recipient mice after 16 h was analyzed by flow cytometry (Dykstra *et al.*, 2011; Florian *et al.*, 2012).

#### **Intracellular pH determination in HSPCs**

Measurement of pH<sub>i</sub> for hematopoietic cells was performed according to Rich *et al.* (2000). HSPC staining was performed first as per standard protocol (see above), and then snarf-1 staining was performed. Briefly, intracellular pH was measured by both flow cytometry by incubating  $2 \times 10^6$  low-density mononuclear cells with a final concentration of 1  $\mu\text{mol/l}$  *carboxy seminaphthorhodafluor-1-acetoxymethylester*, acetate (carboxy SNARF-1 AM; Molecular Probes, Eugene, OR) for 20 min at 37°C. The cells were washed twice with bicarbonate-free buffer, PBS. After SNARF labeling, aliquots of cell suspensions were resuspended in a high K<sup>+</sup>-containing buffer (140 mM KCl, 1 mM MgCl<sub>2</sub>, 2 mM CaCl<sub>2</sub>, 5 mM glucose) at a specific pH usually 6.8, 7.0, 7.2, 7.4, 7.6, and 7.8 for flow cytometry. The calibration curve was performed using the “nigericin, H<sup>+</sup>/K<sup>+</sup> antiporter (2  $\mu\text{g/ml}$ ) that allows the exchange of H<sup>+</sup> for K<sup>+</sup> ions by abolishing the pH gradient across the cell membrane. Fifty thousand events were acquired on a Canto III flow cytometer (Becton Dickinson) and the ratio of the SNARF-1 emission wavelengths 640/580 nm was used to estimate the pH<sub>i</sub> from a calibration curve using Prism 5 software, from which the sample pH<sub>i</sub> values were determined. As diverse hematopoietic cells provide variable SNARF-1 fluorescence, cell-specific standard curves were used to calculate intracellular pH in particular cell types.

#### **IF staining**

Sorted murine HSCs were seeded on fibronectin-coated glass coverslips for 3 h. Cells were fixed, permeabilized (Cytotfix/Cytoperm, BDBiosciences), and blocked with 10% Donkey Serum. Primary antibodies for LAMP2 (GL2A7 Abcam ab13524) and LC3A/B (Cell Signaling Technologies #4108) were incubated overnight at 4°C, followed by secondary fluorescence conjugated antibody incubation at room temperature for 1 h. Post staining with DAPI, slides were mounted. Samples were imaged with a Nikon confocal microscope A1R system (Nikon) equipped with a 60 $\times$  PH objective. Cell volume was measured in NIS software. LC3 and LAMP2 data were analyzed in Z stack-derived 3D images of cells (Florian *et al.*, 2012).

#### **Cell size, reactive oxygen species, and proliferation analysis**

Cell size and volume were determined using a Cellometer Vision CBA microscope, flow cytometer, and confocal analyses. For reactive oxygen species (ROS) and superoxide estimation, cells were incubated with DCF-DA (5  $\mu\text{M}$ , Invitrogen-Molecular probes) in the dark for 30 min at 37°C. Then stained cells were analyzed using a CantoIII flow cytometer (BD Biosciences). To analyze cell cycle and proliferation of HSCs Click-iT Plus EdU Alexa Fluor 488 Flow Cytometry Assay Kit (Thermo Fisher) was utilized according to manufacturer instructions. LT-HSCs (1,000 cells) in U bottom 96 well plates after pH treatment were incubated with 10  $\mu\text{M}$  EdU for 90 min at 37°C (5% CO<sub>2</sub>, 3% O<sub>2</sub>) conditions. After fixation, cells were stained using click reaction and nuclear stain as per manufacturer instructions.

#### **Transmission electron microscopy**

HSCs untreated or upon treatment ( $1.5 \times 10^4$  cells) were fixed with 3% paraformaldehyde, 2.5% glutaraldehyde in 0.1 M cacodylate

buffer. The cells were stained using Evans blue and preembedded in agarose in a small microcentrifuge tube, then post fixed in 1% osmium tetroxide. Samples were further processed for dehydration in graded ethanol solutions, infiltration and embedding into LX-112 resin. The samples were transferred and polymerized in pyramid tip mold (Ted Pella; 10585). Ultrathin sections (70–100 nm) were cut using an ultramicrotome (Leica EM UC7) and collected on 200 mesh grids. The grids were stained with 1% uranyl acetate followed by Reynolds lead citrate. Sections were examined with a Hitachi model H-7650 electron microscope, at 80 KV, equipped with AMT-600 image capture engine software as previously described (Kumar *et al.*, 2014).

#### **Expression analyses and RNASeq analysis**

For expression analyses, RNA was isolated using RNeasy Micro Kit (QIAGEN) from 5,000 pH treated HSCs followed by complementary DNA synthesis using the high-capacity cDNA reverse transcription Kit (Applied Biosystems). Real-time quantitative polymerase chain reaction (PCR) was performed using Taqman PCR Master Mix reagent in triplicate in an ABI Prism 7700 Sequence Detector using (Applied Biosystems). SMART-Seq v4 Ultra Low Input RNA kit (Clontech) was used for cDNA synthesis and amplification from 100 LT-HSCs. Libraries were prepared with Illumina's Nextera XT DNA Library Preparation kit as per Illumina's instruction. Sequencing was done in a Hi-Seq 2500 under paired end 75 bp sequencing conditions. Log<sub>2</sub> values were used to cluster all the DEGs in Cluster 3.0 using uncentered correlation and the complete linkage method.

#### **Mitochondrial function and metabolomics analysis**

Sorted  $4 \times 10^4$  LSKs (Lin<sup>-</sup>c-Kit<sup>+</sup>Sca-1<sup>+</sup>) were treated with pH 6.9 or pH 7.4 conditions. After treatments, mitochondrial functions were performed using the Seahorse XF96 analyzer (Seahorse Bioscience Inc.) and the XF Cell Mito Stress Test Kit according to manufacturer's instructions. For metabolomics, HSCs (5,000 cells) were exposed to pH conditions. The cells were washed twice with PBS, pooled, and collected in a volume of 20  $\mu\text{l}$  and frozen in liquid nitrogen. LC-MS analyses were performed as previously described (Reisz & D'Alessandro, 2017). For LC-MS analysis, the cells were resuspended in an ice-cold organic solution for cell lysis and extraction of metabolites. The organic solvents were dried off and resuspended in an aqueous buffer for LC-MS, as previously described (Reisz & D'Alessandro, 2017).

#### **Measurement of BM pH using multiphoton intravital microscopy**

For detection of pH heterogeneity in BM, we utilized the pH sensitive probe 8-hydroxypyrene-1,3,6-trisulphonic acid (HPTS) and a protocol for multiphoton intravital microscopy adopted from Ray *et al.* (2012). Calibration of HPTS against distinct pH solutions was performed using the 2-photon system at different wavelengths ranging from 700 to 1,000 nm using high power NIR Ti: Sapphire laser at 37 °C *in vitro*. To this end, a variable thick central channel was created using parafilm and coverslips; known pH buffers containing 100  $\mu\text{M}$  or 1 mM HPTS were imaged at different wavelengths using the 2-photon system. To further estimate the pH drift *in vivo* in BM environments, effects of high protein content using FBS, salt (300 mM NaCl), or CaCl<sub>2</sub> were investigated, which showed no major impact of possible interference factors under *in vivo* settings.

For *in vivo* BM pH measurements, mice were anesthetized using ketamine and xylazine and injected retro-orbitally with HPTS (40 mg/kg, Invitrogen) and 70 kDa Rhodamine B–dextran (20 mg/kg, ThermoFisher) to detect pH and blood vessels, respectively. Long bones were carefully exposed, and muscles were carefully cleaned. The mouse was placed on a heated stage, and long bones were mounted on customized stages. Further bone tissue was cautiously trimmed with an electric drill (Dremel) to get better excess of the BM cavity for imaging by leaving a very thin (~30–40  $\mu\text{m}$ ) layer of bone tissue. Multiphoton microscopy on the long bones (femur and tibia) was subsequently performed using a Nikon A1R Multiphoton Upright Confocal Microscope equipped with Coherent Chameleon II Ti:Sapphire IR laser, tuneable from 700 to 1,000 nm and signal were detected by a low-noise Hamamatsu photomultiplier (PMT) tube. Bone tissue was identified as second-harmonic (SHG) signal (PMT). Bones were imaged in PBS using a 25 $\times$  Apo 1.1 NA LWD water Immersion objective and NIS image software. For initial standardization, bones were scanned at wavelength of 700–950 nm detecting HPTS (at an excitation of 530 nm and using a 525/50 filter for detection) and Rhodamine B–dextran (excitation at 580 nm using a 575/25 filter for detection). We then scanned a series of excitation wavelengths ranging from 750 to 900 nm for the detection of the emission of the HPTS signal and used detection filters of 525/50 and 575/25 (Fig 1C). The signal for HPTS was at a maximum at an excitation of 850 nm and detection with a 525/50 filter. Similarly, good signals for TRITC dextran and the SHG signal together were observed at an excitation of 920 nm with a detection with a 575/25 filter as well as an excitation at 850 nm and a 450/50 filter for detection. Instead then using multiple scans using three different excitation wavelengths that would be required to scan bones in ~35 steps of 4  $\mu\text{m}$  down to 120–150  $\mu\text{m}$ , we focused on the best setting in our hands to work with just one excitation wavelength (850 nm) for the excitation of SHG, green (HPTS) and red (TRITC Dextran) fluorescence signals and used detection filters 450/50 (range is thus 475–425 and thus just within the SHG signal of 425), and 525/50 and 575/25 filters, respectively. Importantly, this setting provided us with the best signal intensity for HPTS (most important for present study) and reasonable detection signal levels for SHG and TRITC-Dextran. We imaged 500  $\times$  500- $\mu\text{m}$  areas scanned in ~35 steps of 4  $\mu\text{m}$  down to 120–150  $\mu\text{m}$  depth. Control C57BL/6 mice were used as a negative control for HPTS staining in the bone marrow. Different region of interests (ROI) were analyzed for HPTS ratio, and data represent corresponding pH values based on standard curve. For quantification of the ratio of HPTS fluorescence intensity in the green channel (detection with a 525/50 filter) at 850 vs. 750 nm was plotted by the NIS software using the line of interest.

#### Measurement of HSC apoptosis and death under culture conditions

Murine LT-HSC cells (1,000 cells) or human HSPCs (5,000 cells for apoptosis/death assay, 100 HSPCs for the colony imaging in Fig EV5D) were cultured in IMDM medium or in STEMspan SFEM medium and cytokines with distinct pH or in the presence of DFMO for 2–6 days. For the analysis of the frequency of apoptotic cells, cells were incubated with Annexin V-PE (BD Biosciences) in calcium-containing buffer in the dark for 30 min. For loss of cell membrane integrity, cell impermeable nuclear binding dye 7AAD (1  $\mu\text{g}/\text{ml}$ ) was used. Cells positive for Annexin V<sup>+</sup> but not for 7AAD

are scored as apoptotic cells, while dead cells show both Annexin V<sup>+</sup> and 7AAD<sup>+</sup> (CantoIII flow cytometer (BD Biosciences)).

#### Statistics

All data presented are means  $\pm$  SE, and scatter dot plots depict the mean with error bars representing standard error (SE), until mentioned otherwise. Mice were randomly assigned to different experimental groups. The group sizes ( $n$ ), including biological or technical replicates, specific statistical tests used to determine significance, and  $P$  values are provided in the figure legends.  $P$ -values < 0.05 were considered statistically significant. All statistical analyses were performed using GraphPad prism 7.0 software.

## Data availability

The RNA-Seq data sets produced in this study are available in the following databases: Gene Expression Omnibus GSE225267 (<https://www.ncbi.nlm.nih.gov/geo/query/acc.cgi?acc=GSE225267>).

**Expanded View** for this article is available [online](#).

#### Acknowledgements

We thank Matthew Kofron for advice and critical support with confocal microscopy and pH measurement experiments using intra-vital imaging. SK acknowledges support from ECR/2017/001274 grant provided by Science and Engineering Research Board (SERB) and Ramalingaswami fellowship BT/RLF/Re-entry/28/2014 from Department of Biotechnology (DBT), India. This work is supported by DFG SFB 1074 and SFB 1506. We acknowledge Jeff Bailey and Victoria Summey from CCHMC Comprehensive Mouse and Cancer Core for their help with transplantation experiments and animal work. We thank the Research Flow Cytometry Core and Pathology Core at CCHMC and the Flow Core at Ulm University for support with cell sorting, FACS analyzers and electron microscopy studies. We also thank Medhanie Mulaw for support with RNA Seq data GEO accession, GSE225267. Open Access funding enabled and organized by ProjektDEAL.

#### Author contributions

**Sachin Kumar:** Conceptualization; data curation; formal analysis; supervision; investigation; visualization; methodology; writing – original draft; project administration; writing – review and editing. **Jeffrey D Vassallo:** Conceptualization; investigation; methodology; writing – review and editing. **Kalpana J Nattamai:** Data curation; formal analysis; investigation; visualization; methodology; project administration. **Aishlin Hassan:** Data curation; formal analysis; investigation; visualization; methodology; project administration; writing – review and editing. **Rebekah Karns:** Data curation; formal analysis. **Angelika Vollmer:** Formal analysis; investigation; visualization; methodology. **Karin Soller:** Investigation. **Vadim Sakk:** Investigation. **Mehmet Sacma:** Data curation; software; formal analysis; investigation; visualization; methodology. **Trevis Nemkov:** Data curation; formal analysis; investigation; methodology. **Angelo D'Alessandro:** Resources; data curation; formal analysis; supervision; investigation. **Hartmut Geiger:** Conceptualization; resources; supervision; funding acquisition; methodology; writing – original draft; project administration; writing – review and editing.

#### Disclosure and competing interests statement

The authors declare that they have no conflict of interest.

## References

- Allmeroth K, Kim CS, Annibal A, Pouikli A, Koester J, Derisbourg MJ, Andres Chacon-Martinez C, Latza C, Antebi A, Tessarz P et al (2021) N1-acetylspermidine is a determinant of hair follicle stem cell fate. *J Cell Sci* 134: jcs252767
- Arnett T (2003) Regulation of bone cell function by acid-base balance. *Proc Nutr Soc* 62: 511–520
- Busch GL, Schreiber R, Dartsch PC, Volkl H, Vom Dahl S, Haussinger D, Lang F (1994) Involvement of microtubules in the link between cell volume and pH of acidic cellular compartments in rat and human hepatocytes. *Proc Natl Acad Sci USA* 91: 9165–9169
- Casey JR, Grinstein S, Orłowski J (2010) Sensors and regulators of intracellular pH. *Nat Rev Mol Cell Biol* 11: 50–61
- Damaghi M, Wojtkowiak JW, Gillies RJ (2013) pH sensing and regulation in cancer. *Front Physiol* 4: 370
- Dever TE, Ivanov IP (2018) Roles of polyamines in translation. *J Biol Chem* 293: 18719–18729
- Dykstra B, Olthof S, Schreuder J, Ritsema M, de Haan G (2011) Clonal analysis reveals multiple functional defects of aged murine hematopoietic stem cells. *J Exp Med* 208: 2691–2703
- Eisenberg T, Knauer H, Schauer A, Buttner S, Ruckenstein C, Carmona-Gutierrez D, Ring J, Schroeder S, Magnes C, Antonacci L et al (2009) Induction of autophagy by spermidine promotes longevity. *Nat Cell Biol* 11: 1305–1314
- Florian MC, Dorr K, Niebel A, Daria D, Schrezenmeier H, Rojewski M, Filippi MD, Hasenberg A, Gunzer M, Scharffetter-Kochanek K et al (2012) Cdc42 activity regulates hematopoietic stem cell aging and rejuvenation. *Cell Stem Cell* 10: 520–530
- Hevehan DL, Papoutsakis ET, Miller WM (2000) Physiologically significant effects of pH and oxygen tension on granulopoiesis. *Exp Hematol* 28: 267–275
- Hughes AL, Gottschling DE (2012) An early age increase in vacuolar pH limits mitochondrial function and lifespan in yeast. *Nature* 492: 261–265
- Ito K, Suda T (2014) Metabolic requirements for the maintenance of self-renewing stem cells. *Nat Rev Mol Cell Biol* 15: 243–256
- Ito K, Hirao A, Arai F, Takubo K, Matsuoka S, Miyamoto K, Ohmura M, Naka K, Hosokawa K, Ikeda Y et al (2006) Reactive oxygen species act through p38 MAPK to limit the lifespan of hematopoietic stem cells. *Nat Med* 12: 446–451
- James C, Zhao TY, Rahim A, Saxena P, Muthalif NA, Uemura T, Tsuneyoshi N, Ong S, Igarashi K, Lim CY et al (2018) MINDY1 is a downstream target of the polyamines and promotes embryonic stem cell self-renewal. *Stem Cells* 36: 1170–1178
- Jang YY, Sharkis SJ (2007) A low level of reactive oxygen species selects for primitive hematopoietic stem cells that may reside in the low-oxygenic niche. *Blood* 110: 3056–3063
- Jin G, Xu C, Zhang X, Long J, Rezaeian AH, Liu C, Furth ME, Kridel S, Pasche B, Bian XW et al (2018) Atad3a suppresses Pink1-dependent mitophagy to maintain homeostasis of hematopoietic progenitor cells. *Nat Immunol* 19: 29–40
- Khatib-Massalha E, Bhattacharya S, Massalha H, Biram A, Golan K, Kollet O, Kumari A, Avemaria F, Petrovich-Kopitman E, Gur-Cohen S et al (2020) Lactate released by inflammatory bone marrow neutrophils induces their mobilization via endothelial GPR81 signaling. *Nat Commun* 11: 3547
- Kohler S, Schmoller KM, Crevenna AH, Bausch AR (2012) Regulating contractility of the actomyosin cytoskeleton by pH. *Cell Rep* 2: 433–439
- Kumar S, Geiger H (2017) HSC niche biology and HSC expansion ex vivo. *Trends Mol Med* 23: 799–819
- Kumar S, Ciralo G, Hinge A, Filippi MD (2014) An efficient and reproducible process for transmission electron microscopy (TEM) of rare cell populations. *J Immunol Methods* 404: 87–90
- Kumar S, Nattamai KJ, Hassan A, Amoah A, Karns R, Zhang C, Liang Y, Shimamura A, Florian MC, Bissels U et al (2021) Repolarization of HSC attenuates HSCs failure in Shwachman-diamond syndrome. *Leukemia* 35: 1751–1762
- Lengefeld J, Cheng CW, Maretich P, Blair M, Hagen H, McReynolds MR, Sullivan E, Majors K, Roberts C, Kang JH et al (2021) Cell size is a determinant of stem cell potential during aging. *Sci Adv* 7: eabk0271
- Liu Y, White KA, Barber DL (2020) Intracellular pH regulates cancer and stem cell behaviors: a protein dynamics perspective. *Front Oncol* 10: 1401
- McAdams TA, Miller WM, Papoutsakis ET (1997) Variations in culture pH affect the cloning efficiency and differentiation of progenitor cells in ex vivo haemopoiesis. *Br J Haematol* 97: 889–895
- McAdams TA, Miller WM, Papoutsakis ET (1998) pH is a potent modulator of erythroid differentiation. *Br J Haematol* 103: 317–325
- Mendelson A, Frenette PS (2014) Hematopoietic stem cell niche maintenance during homeostasis and regeneration. *Nat Med* 20: 833–846
- Miettinen JA, Salonen RJ, Ylitalo K, Niemela M, Kervinen K, Saily M, Koistinen P, Savolainen ER, Makikallio TH, Huikuri HV et al (2012) The effect of bone marrow microenvironment on the functional properties of the therapeutic bone marrow-derived cells in patients with acute myocardial infarction. *J Transl Med* 10: 66
- Miller-Fleming L, Olin-Sandoval V, Campbell K, Ralser M (2015) Remaining mysteries of molecular biology: the role of polyamines in the cell. *J Mol Biol* 427: 3389–3406
- Miska J, Rashidi A, Lee-Chang C, Gao P, Lopez-Rosas A, Zhang P, Burga R, Castro B, Xiao T, Han Y et al (2021) Polyamines drive myeloid cell survival by buffering intracellular pH to promote immunosuppression in glioblastoma. *Sci Adv* 7: eabc8929
- Morgan RA, Gray D, Lomova A, Kohn DB (2017) Hematopoietic stem cell gene therapy: progress and lessons learned. *Cell Stem Cell* 21: 574–590
- Mortensen BT, Jensen PO, Helledie N, Iversen PO, Ralfkiaer E, Larsen JK, Madsen MT (1998) Changing bone marrow micro-environment during development of acute myeloid leukaemia in rats. *Br J Haematol* 102: 458–464
- Norddahl GL, Pronk CJ, Wahlestedt M, Sten G, Nygren JM, Ugale A, Sigvardsson M, Bryder D (2011) Accumulating mitochondrial DNA mutations drive premature hematopoietic aging phenotypes distinct from physiological stem cell aging. *Cell Stem Cell* 8: 499–510
- Padda J, Khalid K, Kakani V, Cooper AC, Jean-Charles G (2021) Metabolic acidosis in leukemia. *Cureus* 13: e17732
- Puleston DJ, Baixeli F, Sanin DE, Edwards-Hicks J, Villa M, Kabat AM, Kaminski MM, Stanckzak M, Weiss HJ, Grzes KM et al (2021) Polyamine metabolism is a central determinant of helper T cell lineage fidelity. *Cell* 184: 4186–4202
- Ray A, Lee YE, Kim G, Kopelman R (2012) Two-photon fluorescence imaging super-enhanced by multishell nanophotonic particles, with application to subcellular pH. *Small* 8: 2213–2221
- Reisz JA, D'Alessandro A (2017) Measurement of metabolic fluxes using stable isotope tracers in whole animals and human patients. *Curr Opin Clin Nutr Metab Care* 20: 366–374
- Reshetnyak YK, Moshnikova A, Andreev OA, Engelman DM (2020) Targeting acidic diseased tissues by pH-triggered membrane-associated peptide folding. *Front Bioeng Biotechnol* 8: 335
- Ribeil JA, Haccin-Bey-Abina S, Payen E, Magnani A, Semeraro M, Magrin E, Caccavelli L, Neven B, Bourget P, El Nemer W et al (2017) Gene therapy in a patient with sickle cell disease. *N Engl J Med* 376: 848–855



- Rich IN, Worthington-White D, Garden OA, Musk P (2000) Apoptosis of leukemic cells accompanies reduction in intracellular pH after targeted inhibition of the Na(+)/H(+) exchanger. *Blood* 95: 1427–1434
- Rossi L, Lin KK, Boles NC, Yang L, King KY, Jeong M, Mayle A, Goodell MA (2012) Less is more: unveiling the functional core of hematopoietic stem cells through knockout mice. *Cell Stem Cell* 11: 302–317
- Ryan MA, Nattamai KJ, Xing E, Schleimer D, Daria D, Sengupta A, Kohler A, Liu W, Gunzer M, Jansen M et al (2010) Pharmacological inhibition of EGFR signaling enhances G-CSF-induced hematopoietic stem cell mobilization. *Nat Med* 16: 1141–1146
- Sanderson SM, Gao X, Dai Z, Locasale JW (2019) Methionine metabolism in health and cancer: a nexus of diet and precision medicine. *Nat Rev Cancer* 19: 625–637
- Seita J, Weissman IL (2010) Hematopoietic stem cell: self-renewal versus differentiation. *Wiley Interdiscip Rev Syst Biol Med* 2: 640–653
- Selivanov VA, Zeak JA, Roca J, Cascante M, Trucco M, Votyakova TV (2008) The role of external and matrix pH in mitochondrial reactive oxygen species generation. *J Biol Chem* 283: 29292–29300
- Simsek T, Kocabas F, Zheng J, Deberardinis RJ, Mahmoud AI, Olson EN, Schneider JW, Zhang CC, Sadek HA (2010) The distinct metabolic profile of hematopoietic stem cells reflects their location in a hypoxic niche. *Cell Stem Cell* 7: 380–390
- Suda T, Takubo K, Semenza GL (2011) Metabolic regulation of hematopoietic stem cells in the hypoxic niche. *Cell Stem Cell* 9: 298–310
- Takubo K, Goda N, Yamada W, Iriuchishima H, Ikeda E, Kubota Y, Shima H, Johnson RS, Hirao A, Suematsu M et al (2010) Regulation of the HIF-1 $\alpha$  level is essential for hematopoietic stem cells. *Cell Stem Cell* 7: 391–402
- Ulmschneider B, Grillo-Hill BK, Benitez M, Azimova DR, Barber DL, Nystul TG (2016) Increased intracellular pH is necessary for adult epithelial and embryonic stem cell differentiation. *J Cell Biol* 215: 345–355
- Unnisa Z, Clark JP, Roychoudhury J, Thomas E, Tessarollo L, Copeland NG, Jenkins NA, Grimes HL, Kumar AR (2012) Meis1 preserves hematopoietic stem cells in mice by limiting oxidative stress. *Blood* 120: 4973–4981
- Wang YH, Israelsen WJ, Lee D, Yu VW, Jeanson NT, Clish CB, Cantley LC, Vander Heiden MG, Scadden DT (2014) Cell-state-specific metabolic dependency in hematopoiesis and leukemogenesis. *Cell* 158: 1309–1323
- Yang H, Miller WM, Papoutsakis ET (2002) Higher pH promotes megakaryocytic maturation and apoptosis. *Stem Cells* 20: 320–328
- Yu WM, Liu X, Shen J, Jovanovic O, Pohl EE, Gerson SL, Finkel T, Broxmeyer HE, Qu CK (2013) Metabolic regulation by the mitochondrial phosphatase PTPMT1 is required for hematopoietic stem cell differentiation. *Cell Stem Cell* 12: 62–74
- Zhen A, Carrillo MA, Mu W, Rezek V, Martin H, Hamid P, Chen ISY, Yang OO, Zack JA, Kitchen SG (2021) Robust CAR-T memory formation and function via hematopoietic stem cell delivery. *PLoS Pathog* 17: e1009404



**License:** This is an open access article under the terms of the [Creative Commons Attribution-NonCommercial-NoDerivs](https://creativecommons.org/licenses/by-nc-nd/4.0/) License, which permits use and distribution in any medium, provided the original work is properly cited, the use is non-commercial and no modifications or adaptations are made.